

This article was downloaded by:

On: 14 January 2011

Access details: *Access Details: Free Access*

Publisher *Taylor & Francis*

Informa Ltd Registered in England and Wales Registered Number: 1072954 Registered office: Mortimer House, 37-41 Mortimer Street, London W1T 3JH, UK



Molecular Simulation

Publication details, including instructions for authors and subscription information:

<http://www.informaworld.com/smpp/title~content=t713644482>

Molecular Dynamics Simulation of a Rising Bubble

Mitsuhiro Matsumoto^a; Takahiro Matsuura^a

^a Department of Engineering Physics and Mechanics, Kyoto University, Kyoto, Japan

To cite this Article Matsumoto, Mitsuhiro and Matsuura, Takahiro(2004) 'Molecular Dynamics Simulation of a Rising Bubble', *Molecular Simulation*, 30: 13, 853 — 859

To link to this Article: DOI: 10.1080/08927020412331317467

URL: <http://dx.doi.org/10.1080/08927020412331317467>

PLEASE SCROLL DOWN FOR ARTICLE

Full terms and conditions of use: <http://www.informaworld.com/terms-and-conditions-of-access.pdf>

This article may be used for research, teaching and private study purposes. Any substantial or systematic reproduction, re-distribution, re-selling, loan or sub-licensing, systematic supply or distribution in any form to anyone is expressly forbidden.

The publisher does not give any warranty express or implied or make any representation that the contents will be complete or accurate or up to date. The accuracy of any instructions, formulae and drug doses should be independently verified with primary sources. The publisher shall not be liable for any loss, actions, claims, proceedings, demand or costs or damages whatsoever or howsoever caused arising directly or indirectly in connection with or arising out of the use of this material.

Molecular Dynamics Simulation of a Rising Bubble

MITSUHIRO MATSUMOTO* and TAKAHIRO MATSUURA

Department of Engineering Physics and Mechanics, Kyoto University, Kyoto 606-8501, Japan

(Received January 2004; In final form September 2004)

A large-scale molecular dynamics (MD) simulation was done to investigate the effects of surface adsorption on a bubble moving in a uniform force field. The liquid consists of 2,00,000 Lennard-Jones particles, and surfactants are newly modeled as two sites of Lennard-Jones type combined with a hard harmonic spring. In pure liquid, the flow around the bubble has some finite velocity on the bubble surface, which is consistent with the slip boundary condition assumed in continuum fluid mechanics, and the terminal velocity of the bubble agrees well with the theoretical prediction. When sufficient amount of surfactants are adsorbed on the bubble surface, no flow is observed on the bubble surface as expected, and the terminal velocity drastically decreases. The adsorbed surfactants are transported on the bubble surface and pile up on the rear end of the bubble.

Keywords: Bubble dynamics; Molecular dynamics; Surface adsorption; Micelle

INTRODUCTION

Bubble motions in liquid are strongly affected by the properties of the bubble surface. A small bubble (typically 1–100 μm in diameter) rising in the gravitation is a simple example. Several seconds after the release, it rises with a constant velocity depending on its size; however, when small amount of alcohol or detergent is added, the velocity drastically decreases. This phenomenon is caused by adsorption on the bubble surface where the adsorbed molecules change the flow near the bubble. Experimental and theoretical studies have been done thoroughly [1,2], and recent numerical calculations based on fluid mechanics successfully trace the dynamic behaviors of bubbles [3,4]; recent progress is reviewed in Ref. [5]. However, from molecular points of view, properties of adsorbed species, such as the rates of adsorption and desorption, diffusion

in bulk liquid and on bubble surface, and adsorbed states in detail, are drastically simplified. There still exists a wide gap between molecular properties of adsorbents and the bubble dynamics based on continuum, or hydrodynamic, models.

We have been trying to examine the effects of surface adsorption on bubble dynamics by using direct molecular dynamics (MD) simulations. In this paper, the first simulation of a rising bubble is reported. Although the system size is very much limited when compared with continuum models, we can examine the flow around the bubble in detail without assumptions about molecular motions. In order to do efficient MD simulations, we first develop a simple adsorbent (surfactant) model in section “Surfactant Model”. Some technical details about the main MD simulation are described in section “Simulation of a Rising Bubble”. Results are shown in 4th section, in some comparison with results of fluid dynamics.

SURFACTANT MODEL

Surfactant molecules in general are amphiphilic, i.e. have both hydrophilic and hydrophobic parts. Hydrophilic parts, such as ionic sites and hydroxyl groups, strongly interact with water via hydrogen bonds, whereas hydrophobic parts such as hydrocarbon chains have weak interactions, causing adsorption on vapor–liquid interface. For our purpose to examine bubble dynamics in liquid, such realistic interactions are too complicated, and a simplified model is required. Many studies, e.g. [6–9], have been reported on very simplified models of surfactant solutions, and we adopt a similar model.

*Corresponding author. E-mail: matsumoto@kues.kyoto-u.ac.jp

Our model is based on the Lennard-Jones (12-6) interaction between i - and j -sites:

$$U_{ij}(r) = 4\epsilon_{ij}[(\sigma_0/r)^{12} - (\sigma_0/r)^6], \quad (1)$$

where r is the distance between the two sites, ϵ_{ij} is the energy parameter depending on the combination of the site species; for simplicity, we use the size parameter σ_0 independent of the species. The interaction is truncated at $r = 2.5\sigma_0$. Also for simplicity, each site has the same mass m_0 .

In our system, the solvent is monatomic liquid, and the energy parameter between solvent particles is chosen to be ϵ_0 . In the following description, we choose m_0 , σ_0 , and ϵ_0 as the unit of mass, length and energy, respectively; the unit of time is then $\tau_0 = [m_0/\epsilon_0]^{1/2}\sigma_0$. Simulations were done in a reduced unit system. To compare the results with realistic systems, however, argon parameters are adopted in some descriptions; $m_0 = 6.63 \times 10^{-26}$ kg, $\sigma_0 = 0.34 \times 10^{-9}$ m, $\epsilon_0 = 1.67 \times 10^{-21}$ J (or $\epsilon_0/k_B = 120$ K, where k_B is the Boltzmann constant), and $\tau_0 = 2.1 \times 10^{-12}$ s. The unit of temperature T is ϵ_0/k_B ; the triple point temperature of the solvent is $T \approx 0.67$. All simulations in this work were done at $T = 0.7$.

The surfactant model consists of two sites (solvophilic and solvophobic) connecting with a harmonic spring:

$$U^{\text{sp}}(r) = \frac{1}{2}k^{\text{sp}}[(r/\sigma_0) - (r_0/\sigma_0)]^2, \quad (2)$$

where k^{sp} is the spring constant and r_0 is the natural length of the spring; we adopt $k^{\text{sp}} = 400\epsilon_0$ and $r_0 = 2.5\sigma_0$, which represents a hard and short spring, roughly corresponding to an alcohol molecule with a short hydrocarbon chain. When compared with more realistic surfactant models such as a rod model and a beads-and-sticks model, this two-site model is so simple that we can save the computation time. However, since there is no interaction between springs and particles, the particles can freely cross the "surfactant chain". We expect that the static properties such as adsorption isotherm are little affected, but the detailed dynamics may depend on models. In this study, however, the adsorption is rather weak ($\Gamma \approx 0.3$ at most; see below), and the "interferences" among surfactants are not very significant.

The energy parameter ϵ_{ij} should be properly chosen for our simulation of a bubble with surface adsorption so that the following conditions are met: (1) the model surfactant has sufficient solubility, i.e. it has a comparatively high cmc (critical micelle concentration), and (2) it has sufficient surface adsorption. We carried out a series of MD simulations with NVE ensemble for a small system (3375 particles, reduced temperature = 0.7) of

TABLE I Energy parameters ϵ_{ij} for the surfactant model

	Liquid	Solvophil.	Solvophob.
Liquid	ϵ_0		
Solvophilic site	$1.5\epsilon_0$	$1.5\epsilon_0$	
Solvophobic site	$0.3\epsilon_0$	$0.3\epsilon_0$	$0.5\epsilon_0$

liquid-vapor interface with various sets of ϵ_{ij} , and finally the set shown in Table I is chosen as suitable parameters. Adsorption behaviors with this parameter set is shown in Fig. 1; the surface tension γ was calculated from the spatial integral of the diagonal elements of the pressure tensor, and the surface adsorption Γ was estimated as the surface excess after determining the Gibbs dividing surface [10]. Up to the bulk concentration $C \approx 0.02$, the surface adsorption increases almost linearly with C , which suggests there is no micelle formation in liquid. Combined with a radial distribution analysis in liquid, we conclude that the cmc of this model surfactant at $T = 0.7$ is $C \approx 0.03$, or 1.3 mol/l in argon units, which is much larger than that of typical surfactants. The saturated value of surface adsorption is $\Gamma \approx 0.3$, or 4×10^{-6} mol/m² in argon unit.

SIMULATION OF A RISING BUBBLE

We confine solvent particles in a rectangular cell. When the cell volume is sufficiently large, a bubble can exist stably. Under a uniform external force field of proper strength, the bubble begins to translate, and reaches a steady state with some terminal velocity. The procedure is simple in principle; however, it brings some serious technical difficulties when applied to an MD simulation.

First, due to limitation of the computer resources, both the system size and the number of run steps are limited. We carried out simulations of 2,00,000

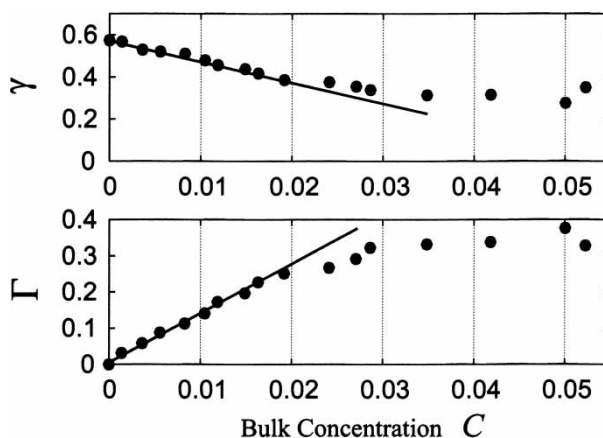


FIGURE 1 Properties of the model surfactant; (top) surface tension γ and (bottom) surface adsorption Γ . The unit is γ in $\epsilon_0\sigma_0^{-3}$ and Γ in σ_0^{-2} , respectively. The lines are a guide for the eye.

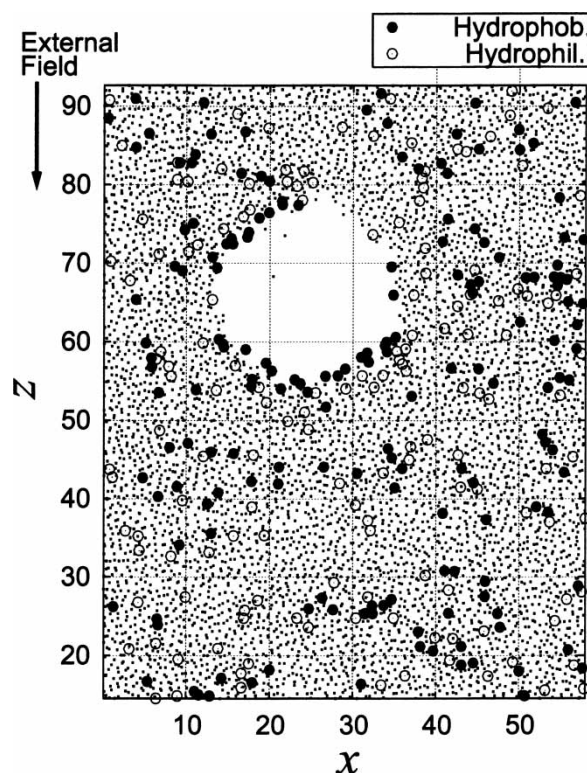


FIGURE 2 Snapshot (cross sectional view) of the bubble in liquid with surfactants.

particles for about one million steps. For that purpose, a parallel MD code with the message passing interface (MPI) library was newly developed, and the simulations were done on a cluster PC system with eight nodes; it takes about 1 s per step. The size of the simulation cell is chosen to be $58.0 \times 58.0 \times 78.0 \sigma_0^3$ in which a bubble of about $20.0 \sigma_0$ (6.8 nm in argon unit) in diameter is confined. Since periodic boundary conditions (PBCs) are used for all directions, the neighboring bubbles are $58.0 \sigma_0$ apart, which may cause a slight interference. A snapshot is shown in Fig. 2.

Second, due to the tiny size of the bubble, an enormously large force field is required. A rough estimation is as follows [4]. The Reynolds number is defined as $Re = \rho V d / \mu$, where V is the bubble velocity in still liquid, d is the bubble diameter, ρ and μ are the density and viscosity of the liquid, respectively. The drag force is expressed with the drag coefficient C_D as $(1/8)C_D \pi \rho V^2 d^2$, which should be equal to the external force in stationary state. In this study, we consider that the external force is proportional to the bubble volume (like the floatation force in the gravitational field). Thus, we obtain

$$\frac{1}{8} C_D \pi \rho V^2 d^2 = \frac{4}{3} \pi a \rho \left(\frac{d}{2}\right)^3, \quad (3)$$

where a is the acceleration due to the external field; the vapor density inside the bubble is neglected for

simplicity. In the case of a bubble in pure liquid (without surface adsorption), C_D is approximated as $16/Re$ in low Re region. Therefore,

$$a = \frac{12\mu V}{\rho d^2}. \quad (4)$$

The bubble diameter d is so small that a huge acceleration a should be chosen to obtain a realistic terminal velocity V . We had to use $a = 0.001 \epsilon_0 \sigma_0^{-1} m_0^{-1}$, which is 7.4×10^{10} larger than the normal gravitational acceleration; the shape of the bubble was still found to be spherical and this extreme field seems to have no artifacts on the bubble dynamics.

Third point is concerning the PBC along the external field (z direction). The direct driving force for the bubble is the buoyancy, or floatation force, which is caused by the density or pressure difference around the bubble. When particles are freely moving in z direction, however, such difference is never generated; the whole system, including particles and the bubble, simply translates along the field. Therefore, we adopt a special boundary condition along z direction, where particles interact each other beyond the basic cell boundary in the same way as the normal PBC, but they never cross the boundary; they are just reflected there, similarly with the reflective boundary condition. In the stationary state, a slight density difference was formed, and the floating motion of the bubble was successfully observed; the density difference between the top and the bottom of the cell was found to be within $\pm 0.2\%$ of the average liquid density. Note that the normal PBC is adopted for other directions (x and y).

The last is the limitation of the cell size along the z direction. The bubble is initially located at the center of the simulation cell; as the bubble translates (or “floats”) to the z direction, however, the special boundary described above may affect its behavior. To overcome this difficulty, we adopt a “cut-and-paste” technique; when the bubble comes close to one end of the cell, we “cut” a part of the cell from another end, and “paste” it there, after slightly expanding the cut part according to the density difference between the top and the bottom parts of the cell. The detailed procedure is as follows. We monitor the center position of the bubble during the simulation; when the bubble translates more than a certain threshold distance Δz along the z direction from the initial position, we cut the downstream end region with thickness Δz of the simulation cell, expand it by factor $\rho_{\text{down}}/\rho_{\text{up}}$ along the z direction, and paste, or joint, it to the upstream end, where ρ_{down} and ρ_{up} are the number density of the solution at each end of the simulation cell. With this procedure, we are able to trace the bubble translation

for distance longer than the cell size. Here we arbitrarily used $\Delta z = 2\sigma_0$.

Other relevant conditions are as follows. The time integration is done by the standard leap frog algorithm with the time step $0.004\tau_0$. The number of particles is 2,00,000; in the case of a bubble with adsorption, 5000 model surfactants are mixed with 1,90,000 solvent particles, the concentration of which is about 0.025. The temperature is controlled to be $0.7\epsilon_0/k_B$ only in the most upstream rectangular region of $2.5\sigma_0$ width by a simple velocity scaling so that there is little disturbance on the flow around the bubble. The particle positions and velocities were stored every 500 steps ($2\tau_0$) for data analysis.

RESULTS AND DISCUSSION

In order to detect the bubble, the simulation cell is divided into a cubic lattice of size $\Delta_l = 0.2\sigma_0$. Each lattice point is defined as "vacant" when there are no particles (either solvent particles or surfactant sites) within the distance $\Delta_c = 2.0\sigma_0$. The bubble is defined as a group of vacant lattice points; similarly, the bubble surface is defined as a group of lattice points adjacent to vacant points. Thus, the center position, the volume, and the surface area, of the bubble are easily estimated. We examined the bubble shape in detail, and found that the bubble is almost spherical, probably due to its tiny size; the relative difference between the longest and the shortest axes is within 1% for the pure liquid system and within 10% for the surfactant solution system; in the latter system, the bubble is slightly collapsed along the z direction.

After 2,00,000–3,00,000 steps (800 – $1200\tau_0$), the system is almost in stationary state. The bubble position along the z axis and the bubble radius (with assuming a spherical shape) are shown in Figs. 3 and 4. In the pure liquid system, the bubble seems to translate with a constant velocity after

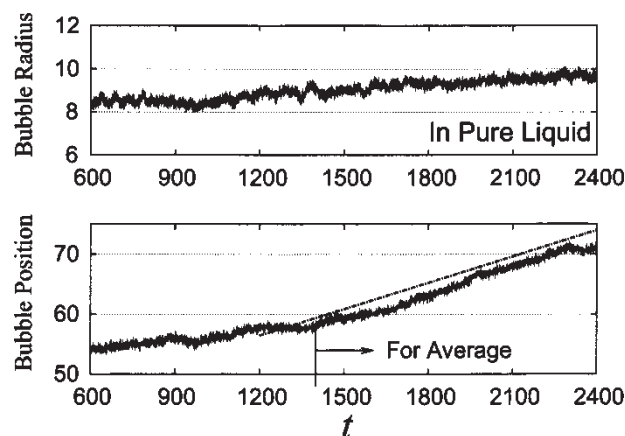


FIGURE 3 Change of the center position (along z axis) and the radius of the bubble in pure liquid; the dashed line shows a motion with constant rising velocity.

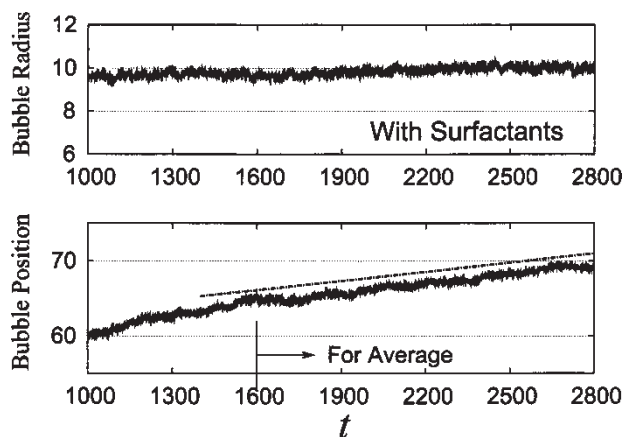


FIGURE 4 Same as Fig. 3 for the bubble with surface adsorption.

$1400\tau_0$. Statistical averages are taken for the period 1400 – $2400\tau_0$ although the bubble size continued to increase slightly. For the surfactant solution system, statistical average are taken for 1600 – $2800\tau_0$.

From the position change, the terminal velocity is estimated as $V = 0.0133\sigma_0\tau_0^{-1}$ (2.11 m/s in argon unit) in the pure liquid, and $0.0042\sigma_0\tau_0^{-1}$ (0.66 m/s) in the surfactant solution; thus the surface adsorption is found to strongly suppress the bubble translation as expected.

It may be interesting to compare this result with a simple theoretical calculation. The Reynolds number estimated with argon parameters ($\rho = 1410 \text{ kg/m}^3$ and $\mu = 0.28 \times 10^{-3} \text{ Pa s}$) is $\text{Re} = 3.68 \times 10^{-3} d/\sigma_0$, where d is the bubble diameter. Since d/σ_0 is about 20 in both systems, the flow is well in a low Reynolds number regime and the Stokes approximation is applicable. For a spherical bubble in incompressible liquid, the terminal velocity is predicted [11] as

$$V_{\text{stokes}} = \frac{\rho}{6\mu} a \left(\frac{d}{2} \right)^2, \quad (5)$$

where the flow slip is assumed on the bubble surface, and the density and the viscosity of the gas in the bubble are neglected. If we choose $d/\sigma_0 = 20$, it gives $V_{\text{stokes}} \approx 1.5 \text{ m/s}$, which is slightly smaller than the MD result, 2.1 m/s. When sufficient surface adsorption exists on the bubble surface, the drag coefficient C_D increases to $24/\text{Re}$ from $16/\text{Re}$, which gives $2/3$ times slower V_{stokes} . If we similarly choose $d/\sigma_0 = 20$, it predicts $V_{\text{stokes}} \approx 1.0 \text{ m/s}$, which is much larger than the MD result, 0.66 m/s. As described later, there is some arbitrariness in the choice of d/σ_0 . However, the large discrepancy in the case of surfactant solution is probably due to the system size limit, i.e. the interference between bubbles in the neighboring cells. The thickness of the boundary layer δ around a solid sphere is useful to demonstrate it. In an incompressible viscous fluid,

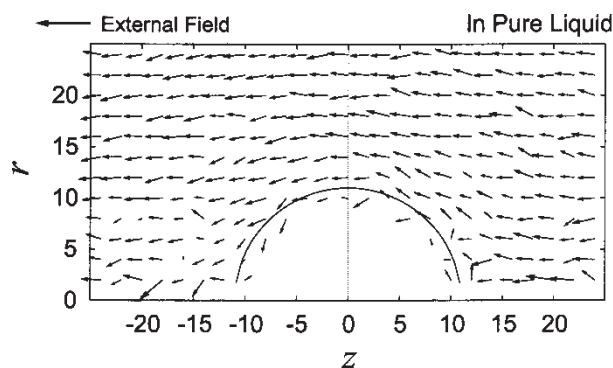


FIGURE 5 Velocity field around the bubble in pure liquid (in cylindrical coordinates). Solid curve roughly shows the bubble surface.

it is estimated as [11]

$$\delta \approx \frac{5}{8} \sqrt{\frac{\mu d}{\rho V}}. \quad (6)$$

In our system of surfactant solution, δ is found to be $170\sigma_0$, much larger than the cell size $58\sigma_0$; thus the flow around the bubble cannot develop well, and the velocity is suppressed. Note that there exists no clear boundary layer in the case of a bubble in pure liquid where the flow slips on the bubble surface.

The detailed flow pattern and the density profiles are examined by taking spatial and temporal average, where we assume a rotational symmetry around the z axis penetrating the bubble center. The results are shown in Figs. 5–6 for the pure liquid system and in Figs. 7–8 for the surfactant solution. As expected, the flow continuously exists, or slips, on the bubble surface in pure liquid. From the contour of solvent density, the averaged bubble surface has some width, similarly to a flat surface [10]; therefore, it is hard to exactly determine the size of a tiny bubble. A simple definition gives the radius $\sim 9.5\sigma_0$ (in Fig. 3), but the flow as far as $12\sigma_0$ may be affected. In the case of surfactant solution, the flow pattern is very disturbed, and the flow speed is almost zero near the bubble surface, which is a strong evidence of

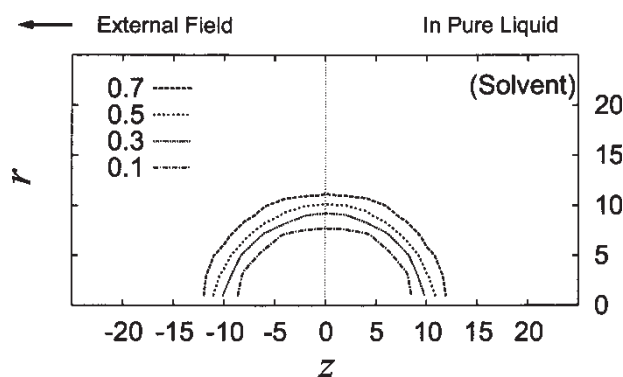


FIGURE 6 Contour of liquid density around the bubble in pure liquid (in cylindrical coordinates).

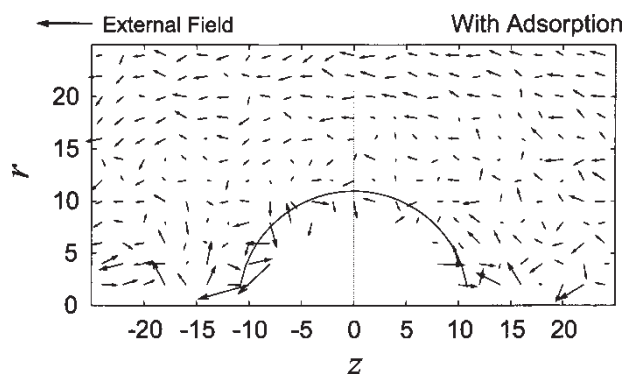


FIGURE 7 Same as Fig. 5 for the bubble with surface adsorption; the arrows are magnified twice than in Fig. 5.

retardation by the surfactant adsorption. Solvent distribution is almost the same as in pure liquid, but the surfactant distribution shows a non-uniform pattern; the surfactants are piled up on the rear (downstream) end of the bubble surface. This roughly corresponds to the “stagnant cap” assumed in theoretical treatments [1–5], but no clear cap edge is observed.

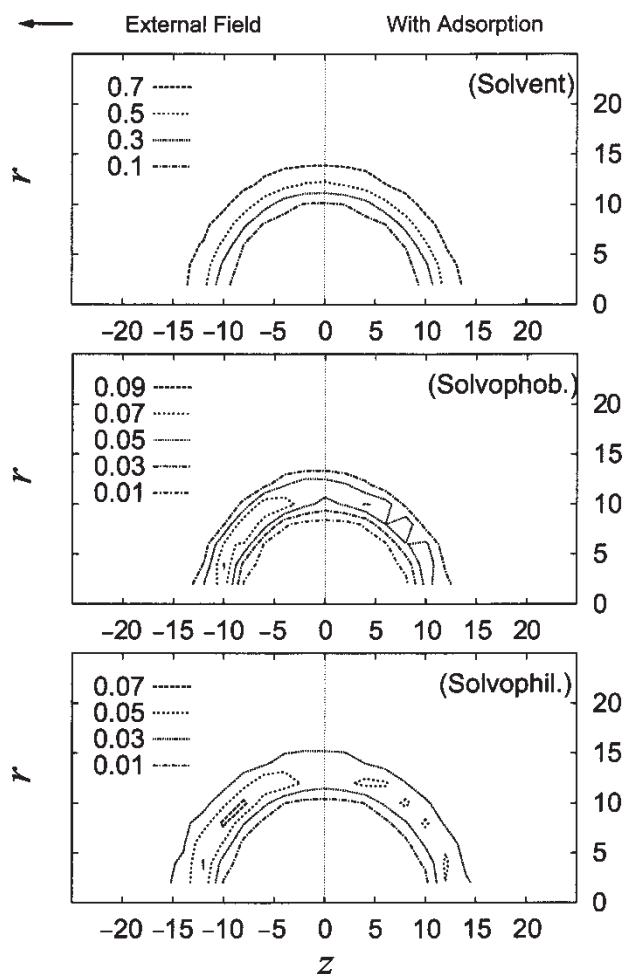


FIGURE 8 Density contours of solvent, solvophobic and solvophilic sites for the bubble with surface adsorption.

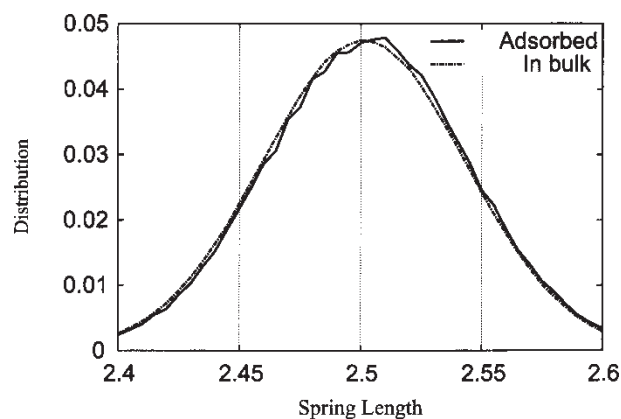


FIGURE 9 Spring length distribution of the surfactants.

On average, 200–300 surfactants are always adsorbed on the bubble surface. This is still insufficient to analyze the spatial distribution of the stress around the bubble, and only the histogram of the spring length of surfactants is calculated (Fig. 9). In the bulk liquid, it shows a reasonable Gaussian distribution around the natural length ($2.5\sigma_0$); the spring of adsorbed surfactants is found to be slightly elongated, because they sustain, or compensate, the stress around the bubble.

Finally, absorption/desorption dynamics is examined. Examples of surfactant trajectories are shown in Fig. 10, where the process is clearly seen that a surfactant is adsorbed, transferred along the bubble surface, and detached from the surface. To estimate the desorption rate, we calculate the survival probability $P(t)$, which is the probability that an initially adsorbed surfactant remains on the surface after the period t . As shown in Fig. 11, $P(t)$ has an exponential decay tail with decay time τ_d . The desorption rate is then estimated as $\tau_d^{-1} \approx 6.2 \times 10^{-4} \tau_0^{-1}$, or $3 \times 10^8 \text{ s}^{-1}$, which is much faster than that of typical surfactants, 10 s^{-1} [3]; the simplified

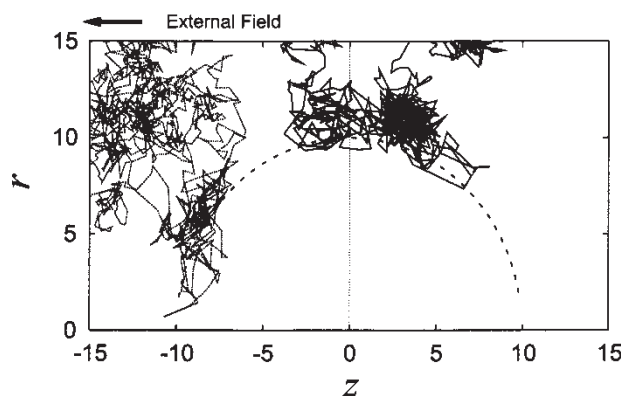


FIGURE 10 Examples of surfactant trajectory around the bubble.

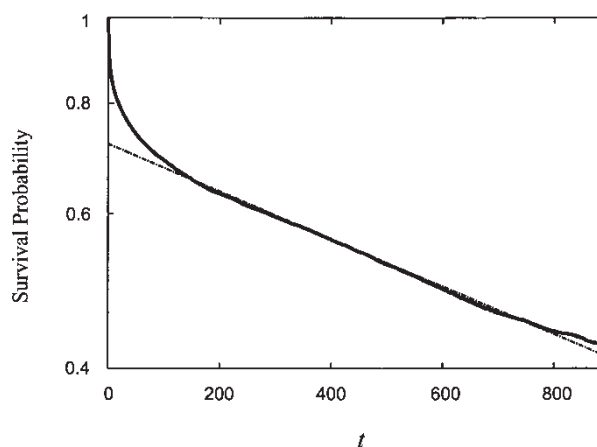


FIGURE 11 Decay of the survival probability of surfactants which were initially adsorbed on the bubble surface. The desorption rate is estimated from the exponential tail shown by the dashed line.

surfactant model and the extreme field may cause this fast desorption, but the detailed dynamics is to be analyzed.

SUMMARY

Using a simplified surfactant model, we investigated the effects of surface adsorption on bubble dynamics with a large-scale MD simulation. The terminal velocity of the bubble without surface adsorption agrees with a hydrodynamic calculation of Stokes flow assuming a slip on the bubble surface. A sufficient amount of surface adsorption strongly suppresses the slip, and the terminal velocity decreases to 1/3 of the slip case. The adsorbed surfactants are piled up on the downstream side of the bubble surface, and the rate of desorption from the surface was estimated.

Acknowledgements

We are grateful to Prof. S. Komori of Kyoto University for stimulating discussion and a financial support by Grants-in-Aid for Scientific Research ((S) 14102016) from Japan Society for the Promotion of Science and by COE Program for Research and Education on Complex Functional Mechanical Systems from the Ministry of Education, Culture, Sports, Science and Technology, Japan.

References

- [1] Harper, J.F. (1973) "On bubbles with small immobile adsorbed films rising in liquids at low Reynolds numbers". *J. Fluid Mech.*, **58**, 539.
- [2] Levan, M.D. and Newman, J. (1976) "The effect of surfactant on the terminal velocities of a bubble or a drop". *AIChE. J.*, **22**, 695.

- [3] Bel Fdhila, R. and Duineveld, P.C. (1996) "The effect of surfactant on the rise of a spherical bubble at high Reynolds and Peclet numbers". *Phys. Fluids*, **8**, 310–321.
- [4] Cuenot, B., Magnaudet, J. and Spennato, B. (1997) "The effects of slightly soluble surfactants on the flow around a spherical bubble". *J. Fluid Mech.*, **339**, 25–53.
- [5] Magnaudet, J. and Eames, I. (2000) "The motion of high-Reynolds-number bubbles". *Ann. Rev. Fluid Mech.*, **32**, 659–728.
- [6] Telo da Gama, M.M. and Gubbins, K.E. (1986) "Adsorption and orientation of amphiphilic molecules at a liquid–liquid interface". *Mol. Phys.*, **59**, 227–239.
- [7] Smit, B. (1988) "Molecular-dynamics simulations of amphiphilic molecules at a liquid–liquid interface". *Phys. Rev. A*, **37**, 3431–3433.
- [8] Rector, D.R., van Swol, F. and Henderson, J.R. (1994) "Simulation of surfactant solutions. 1. Micelle formation in the bulk phase". *Mol. Phys.*, **82**, 1009–1031.
- [9] Tomassone, M.S., Couzis, A., Maldarelli, C.M., Banavar, J.R. and Koplik, J. (2001) "Molecular dynamics simulation of gaseous-liquid phase transitions of soluble and insoluble surfactants at a fluid interface". *J. Chem. Phys.*, **115**, 8634–8642.
- [10] Rowlinson, J.S. and Widom, B. (1982) "Molecular theory of capillarity", Ch. 2–4, Clarendon, New York.
- [11] Landau, L.D. and Lifshitz, E.M. (1987) "Fluid mechanics", Ch. 2. *Course of Theoretical Physics*, 2nd Ed., Vol. 6, Butterworth, Oxford.